Sains Malaysiana 43(6)(2014): 833–842

Characteristics of Nanostructured $Ca_xZn_{(1-x)}Al_2O_4$ Thin Films Prepared by Sol-Gel Method for GPS Patch Antennas

(Ciri Filem Nipis $Ca_xZn_{(1-x)}Al_2O_4$ Berstruktur Nano yang Dihasilkan Melalui Kaedah Sol-Gel untuk GPS Tampalan Antena)

WAN NASARUDIN WAN JALAL, HUDA ABDULLAH*, MOHD SYAFIQ ZULFAKAR, SAHBUDIN SHAARI, MOHAMMAD THARIQUL ISLAM & BADARIAH BAIS

ABSTRACT

$Ca_xZn_{(1-x)}Al_2O_4$ thin films (x = 0.00; 0.05; 0.10; 0.15 and 0.20) were prepared by sol-gel method with the substitution of Zn^{2+} by Ca^{2+} in the framework of $ZnAl_2O_4$. The effect of Ca addition on the structure and morphology of $CaZnAl_2O_4$ thin films was investigated by x-ray diffraction (XRD), field-emission scanning electron microscope (FESEM), energy-dispersive x-ray spectroscopy (EDX), ultra-violet visible (UV-Vis) and atomic force microscope (AFM). The XRD patterns showed the characteristic peaks of face-centred cubic (fcc) $ZnAl_2O_4$ and $CaZnAl_2O_4$. The addition of Ca increased the crystallite size from 8.9 to 30.2 nm. The bandgap of $Ca_xZ_{n(1-x)}Al2O4$ thin film was found in the range of 3.40 to 3.84 eV. SEM micrograph shows the morphology of all thin films is sphere-like, with the grain size increased from 33 to 123 nm. The AFM images show the roughness of surface morphology increased. The substitution of Zn^{2+} by Ca^{2+} increased the crystallite size, grain size and surface roughness which evidently increased the density (4.59 to 4.64 g/cm^3) and dielectric constant (8.48 to 9.54). The composition of $Ca_xZn_{(1-x)}Al_2O_4$ is considered as suitable material for GPS patch antennas.

Keywords: Band gap; Ca-$ZnAl_2O_4$; GPS patch antena; nanostructures

ABSTRAK

Filem nipis $Ca_xZn_{(1-x)}Al_2O_4$(x = 0.00; 0.05; 0.10; 0.15 dan 0.20) telah dihasilkan dengan kaedah sol-gel iaitu menggantikan Zn^{2+} dengan Ca^{2+} di dalam bahan utama $ZnAl_2O_4$. Kesan terhadap penambahan Ca pada struktur dan morfologi filem nipis $CaZnAl_2O_4$ telah dianalisis dengan menggunakan pembelauan sinar-x (XRD), mikroskopi imbasan pancaran medan elektron (FESEM), x-ray serakan tenaga spektroskopi (EDX), cahaya nampak ultra lembayung (UV-Vis) dan mikroskopi daya atomik (AFM). Corak pembelauan XRD menunjukkan ciri-ciri puncak berpusat muka padu pada bahan $ZnAl_2O_4$ dan $CaZnAl_2O_4$. Penambahan Ca telah meningkatkan saiz kristal daripada 8.9 kepada 30.2 nm. Jalur tenaga bagi filem nipis $Ca_xZn_{(1-x)}Al_2O_4$ ialah antara 3.40 hingga 3.84 eV. Graf mikro SEM menunjukkan morfologi bagi kesemua filem nipis adalah berbentuk butiran dengan saiz butiran meningkat daripada 33 kepada 123 nm. Imej AFM menunjukkan berlakunya peningkatan pada permukaan morfologi $Ca_xZn_{(1-x)}Al_2O_4$. Penggantian Zn^{2+} dengan Ca^{2+} telah meningkatkan saiz butiran dan peningkatan kekasaran permukaan yang seterusnya memberi kesan terhadap ketumpatan bahan (4.59 kepada 4.64 g/cm^3) dan pemalar dielektrik (8.48 kepada 9.54). Komposisi $Ca_xZn_{(1-x)}Al_2O_4$ dianggap sebagai bahan yang sesuai untuk penghasilan GPS tampalan antena.

Kata kunci: Ca-$ZnAl_2O_4$; GPS tampalan antena; jalurtenaga; strukturnano

INTRODUCTION

In recent years, spinel-type zinc aluminate ($ZnAl_2O_4$) ceramics has become technologically important due to their unique properties. These materials are important in many applications due to their synergetic advantages such as high stability, low temperature sinterability, high thermal resistance, high mechanical strength and wide bandgap (Saberi et al. 2008; Tawatchai et al. 2009; Thinesh Kumar et al. 2012). The reported bandgap of $ZnAl_2O_4$ is 3.8 eV (Zhang et al. 2012) with the effective transparency at wavelengths above 320 nm. $ZnAl_2O_4$ is already used as UV transparent conductor, sensor, microwave dielectric ceramic material and optical material (Ciupina et al. 2004; Fatemeh & Masoud 2011; Suresh et al. 1999). Furthermore, $ZnAl_2O_4$ has also been used as a microwave dielectric ceramic material in telecommunication industry as resonators, filter or oscillators for wireless FAX, cellular phones, global position satellite (GPS), military radar systems, intelligent transport system (ITS) and direct broadcast satellites. Recently, Lei et al. (2009), Surendran

et al. (2004), Wang et al. (2009) and Wu et al. (2011) have studied the properties of $ZnAl_2O_4$ ceramics doped with TiO_2, $Mg2TiO_4$-$xSrTiO_3$, Co_2TiO_4, and $Mg2TiO_4$, respectively, by conventional solid state reaction method. Accordingly, they have found that, the $ZnAl_2O_4$ ceramics has excellent properties as GPS patch antenna or microwave substrate. However, the miniaturization of GPS patch antenna has become primary issue in the past few years, due to the operating frequency ranges of microwave wireless communications are expanding to millimeter wave applications (Bian et al. 2008; Ye et al. 2009). The needed of new ceramic materials that can reduce the size of GPS components are urgently required. A material with high dielectric constant (ε_r) is required in order to miniaturize GPS patch antenna. However, Huang et al. (2009) and Lei et al. (2011) reported that materials with low dielectric constant (ε_r<15) tend to be more interesting. Low dielectric constant can minimize cross-coupling with conductors and shorten the time for the electronic signal transition and having high quality factor (Lei et al. 2011).

Therefore, zinc aluminate ($ZnAl_2O_4$) was selected due to low dielectric constant (ε_r ~8.5) among the spinel-type and is well known as microwave dielectric ceramics. Narang and Shalini (2010) reported that the structural, morphological and electrical properties of microwave dielectric ceramics can be improved by adding suitable additives or by optimizing the experimental preparation methods. In addition, Thinesh Kumar et al. (2012) also reported, the important factors in order to improve the structural, morphological and electrical properties of $ZnAl_2O_4$ is ceramic materials with metal (conducting) oxides. In fact, the performance of the GPS patch antenna depends on the ceramics properties (Mailadil 2008).

However, there have been no previous studies on $ZnAl_2O_4$ doped with purely alkaline metal ions to use as microwave dielectric ceramics in telecommunication industries. Furthermore, many researchers have reported $ZnAl_2O_4$ doped with other materials for optical and catalytic applications such as Sr (II): $ZnAl_2O_4$ (Thinesh Kumar et al. 2012), $Zn_{1-x}Co_xAl_2O_4$ (Luiz et al. 2009), $Zn_{1-x}MnxAl_2O_4$ (Sanchez et al. 2010), $ZnAl_2O_4$:Eu^{3+} (Renata & Osvaldo 2010) and $ZnAl_2O_4$:TR (TR = Eu^{3+}, Tb^{3+}) (Barros et al. 2006). Meanwhile, calcium (Ca^{2+}) dopant was selected as a purely alkaline metal. It has good characteristic such as high density, hardness, strength and is stable in the service temperature. In addition, Ca^{2+} has technological importance in the application of optical coating material (Rodriguez et al. 2012) like $ZnAl_2O_4$ (Ciupina et al. 2004; Fatemeh & Masoud 2011; Suresh et al. 1999). Based on these properties, Ca^{2+} was selected as a doping material.

The preparation of $Ca_xZn_{(1-x)}Al_2O_4$ microwave dielectric ceramic normally involves heating processes of raw materials in order to control the purity, particle size, particle size distribution and heterogeneity. These factors play an important roles to produce $Ca_xZn_{(1-x)}Al_2O_4$ materials. Therefore, sol gel method was selected as an ideal technique to synthesize $Ca_xZn_{(1-x)}Al_2O_4$ due to the different types of materials and phase compositions (Farley et al. 2003). In addition, from the previous finding of $ZnAl_2O_4$ as microwave dielectric ceramic by Lei et al. (2009), Surendran et al. (2004), Wu et al. (2011) and Wang et al. (2009), there have been no reports on $ZnAl_2O_4$ preparation using sol-gel method.

In order to understand the properties of $CaZnAl_2O_4$ dielectrics, the relationships between structure, morphology, phase compositions and optical properties were investigated. The aim of this paper was to investigate the properties of $ZnAl_2O_4$ thin films doped with calcium (Ca) as GPS patch antennas. Thin films were prepared by substituting Zn^{2+} with Ca^{2+} to form a new nanostructure of $CaZnAl_2O_4$. The effects of substitution of Zn^{2+} by Ca^{2+} were characterized using XRD, FESEM and AFM to investigate the nanostructural, phase compositions and morphological properties. The optical property of $CaZnAl_2O_4$ thin films was also examined. This kind of new ceramic materials could be applied as GPS patch antennas. The synthesis of calcium, aluminium and zinc mixed oxides by sol gel method is being reported in this paper for the first time.

Experimental Details

Sol gel method was used for the synthesis of calcium (Ca) doped $ZnAl_2O_4$ thin films with different molar ratios. Zinc acetate dehydrate ($Zn(O_2CCH_3)_2$), aluminium nitrate nanohydrate ($Al(NO_3)_3 \cdot 9H_2O$) and calcium nitrate ($Ca(NO_3)_2$) were selected as starting raw materials for zinc, aluminum and calcium sources, respectively. The different molar ratios of $Ca_xZn_{(1-x)}Al_2O_4$ raw materials were dissolved in absolute ethanol. Initially aluminium nitrate was dissolved in 60 mL absolute ethanol (C_2H_5OH) as solvent, followed by ethylene glycols (0.5 mL) as the chelating agent to the solution. Calcium nitrate and zinc acetate were added to the solution. After being kept at around 75°C for 1 h, de-ionized water (0.53 mL) was gradually added to hydrolyze the aqueous reactants as the proton donor, followed by nitric acid (CA) with an amount of 0.36 mL are utilized for preparing homogeneous solution. The solution was heated at 75°C with constant stirring using magnetic stirrer for 3 h until it turned into a clear solution. Solutions containing $Ca_xZn_{(1-x)}Al_2O_4$ were stirred continuously for 0.5 h at 180°C in order to obtain transparent and stable sol. $Ca_xZn_{(1-x)}Al_2O_4$ thin films were prepared by spin-coating on to the FTO substrate and treated at the 85°C for 15 min and the procedure was repeated for 10 times to get a good thickness. Finally, the films were annealed at 700°C for 1 h (1°C/min for heating and cooling rate) in ambient atmosphere to eliminating the remaining organic matter (water and oxygen).

The nanostructure of $Ca_xZn_{(1-x)}Al_2O_4$ thin films was characterized by X-ray diffraction (XRD) using CuK_α radiation of λ=1.540600 Å (XRD, Siemens D-500). Data were collected between 20° to 60° (2Å), with a selected step scan mode with a step width of 0.025°. The surface morphologies and chemical compound of films were observed by field-emission scanning electron microscope (FESEM, Zeisz Supra 15 KV), atomic force microscope

(AFM, NTEGRA Prima) and energy-dispersive x-ray spectroscopy (EDX), respectively. The optical property of the films was examined by the absorption spectra using ultra-violet (UV-Vis) spectrometer, in the wavelength range of 200 to 800 nm. The ε_r was measured using an LCR spectrometer (Agilent E4980A).

Results and Discussion

X-ray Diffraction Studies (XRD)

The crystallinity and orientation of nanostructured $Ca_xZn_{(1-x)}Al_2O_4$ thin film were examined by using X-ray diffraction (XRD) after the annealing treatment at 700°C for 1 h as shown in Figure 1. This temperature was set for all the values of x ($x = 0.00, 0.05, 0.10, 0.15$ and 0.20). The characteristic peaks of the $Ca_xZn_{(1-x)}Al_2O_4$ nanostructure were shown, according to the JCPDS files 00-005-0669 and 01-087-0265, for $ZnAl_2O_4$ and $CaZnAl_2O_4$, respectively. The observed diffraction peaks of all samples correspond to the standard pattern of face-centered cubic $ZnAl_2O_4$ with dominant peak (311) at around 36.26° and (220) at 31.7°. Analysis of the XRD pattern depicted the formation of the main crystalline planes (220), (222), (400), (331) (422) and (511) at 2θ = 31.72°, 37.78°, 44.78°, 47.51°,56.64° and 59.34°, respectively and it was proven that (311) is the preferential orientation, as previously reported by Barros et al. 2006. At $x = 0.10$, the highest diffraction peaks observed at (220) due to Ca^{2+} ions may be substitute with the trivalent Al^{3+} ions or divalent Zn^{2+} ions. However, the peak changed back to (311) with the increase of Ca amount. From the most intense peak, only peak (511) was observed for the un-doped Ca ($x = 0.00$).

The peak corresponding to face-centered cubic $CaZnAl_2O_4$ appears at 29.37° (422), when the Ca-content increases up to $x = 0.20$. It was observed that the Ca-added is successfully doped in the $ZnAl_2O_4$ lattice and emerge as the same phases at higher loading. The XRD analyses suggested that the increasing amount of Ca could lead to the increasing intensity of the diffraction peaks of $CaZnAl_2O_4$ and $ZnAl_2O_4$. This analysis confirmed that the peak of $CaZnAl_2O_4$ was formed when x was more than 0.20. However, the peak of $CaZnAl_2O_4$, did not appear very clear due to a small quantity of Ca coated on $ZnAl_2O_4$. Figure 1 also shows the increment of x value whereas the peak shifted to the higher angle, implying the formation of $CaZnAl_2O_4$ thin film. This is because the ionic radii of Ca^{2+} (0.99 nm) (Huang et al. 2009) is larger than Zn^{2+} (0.72 nm) (Chatpong et al. 2013) in $CaZnAl_2O_4$ compound.

The XRD patterns also show that the presence of secondary phases corresponding to the hexagonal ZnO and appear at 34.39° (002). These phenomenons were also explained by Renata and Osvaldo (2010). The formation of the secondary phases was attributed to the formation of vacancies resulting from the incorporation of Ca ions into the host lattice ($ZnAl_2O_4$). The nature of the Ca^{2+} ions doping the nanostructured $ZnAl_2O_4$ spinels appears to be much complex, for it is possible that these ions substitute the trivalent Al^{3+} ions or divalent Zn^{2+} ions.

The crystallite size (D_{hkl}) wes calculated from dominant peak (311) and broadened peaks (311, 220, 400, 331 and 422) of XRD data, based on the Scherrer's equation using the following *hkl* peaks (Tian et al. 2009);

$$D_{hkl} = \frac{\lambda}{\beta \, Cos\,\theta} \, 0.94, \qquad (1)$$

where λ is the X-ray wavelength (0.15418 nm) and β is the full-width at half-maximum intensity of the diffraction line.

The calculated crystallite size of $ZnAl_2O_4$, $Ca_{0.05}Zn_{0.95}Al_2O_4$, $Ca_{0.1}Zn_{0.90}Al_2O_4$, $Ca_{0.15}Zn_{0.85}Al_2O_4$, and $Ca_{0.2}Zn_{0.80}Al_2O_4$ were 8.9, 9.0, 15.7, 21.4 and 30.2 nm, respectively. The increase in the crystallite size was

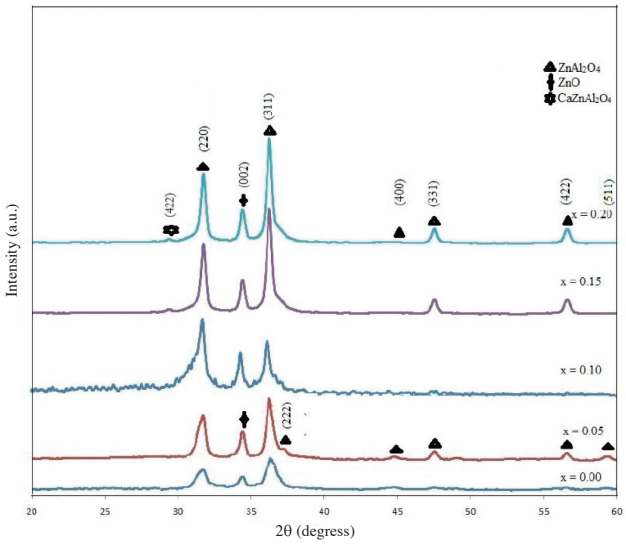

FIGURE 1. XRD patterns of $Ca_xZn_{(1-x)}Al_2O_4$ (x=0.00, 0.05, 0.10, 0.15 and 0.20)

in parallel with Ca loading due to the requirement of high energies for the Ca^{2+} ions. The ions need to enter into the lattice and get substituted for a complete grain crystallization and growth. Furthermore, there must be no other crystalline phases to hinder the growth of Ca-ZnO-Al_2O_3 grains at the grain boundaries.

The structural parameters, lattice parameter (a) and apparent density are listed in Table 1. It has been shown that the crystallite size increased upon Ca-substitution, from 8.98 to 30.16 nm. The lattice parameter of $ZnAl_2O_4$ was calculated based on the X-ray diffraction patterns, using (2) (Ianos et al. 2012):

$$a = d_{hkl} (h^2 + k^2 + l^2). \quad (2)$$

The experimental values of lattice parameters (a) upon the Ca-substitution of Zn decreased from 8.093 to 8.065 Å. The decrease in lattice parameter was due to the peak shifted to the higher angle. The shift of XRD diffraction peaks was indicated that the lattice parameter (a) has changed. These experimental lattice parameters of $ZnAl_2O_4$ are in good agreement with the reported value a = 8.083 to 8.095 Å (Luiz et al. 2009; Zawadzki et al. 2009) and the theoretical value (8.05 Å). However, crystallite size and the lattice parameters show inverse linear relationship with Ca loading (Figure 2). Table 1 also shows that the apparent densities increased with x varied from 0 to 0.20 (4.59 to 4.64 g/cm^3). The density of films was measured by the Archimedes method. Fauzana et al. (2013) reported that, the increase in apparent densities caused by decrease in the number of pores in the nanostructure, as shown in Figure 4. Furthermore, the increase in apparent densities was associated with high dielectric constant and played an important role in controlling the dielectric loss for GPS patch antenna as reported by Chen (2011) and Huang et al. (2009).

UV-VIS ANALYSIS

Figure 3(a) to 3(e) shows the UV-vis absorbance spectra of $Ca_xZn_{(1-x)}Al_2O_4$ thin films after the annealing treatment at 700°C for 1 h. The absorption spectra were recorded in the wavelength range of 200 to 800 nm. The optical band gap energy (E_g) was estimated by the method proposed by Wood and Tauc (1972) (Muhammad et al. 2011);

$$\alpha = \frac{A}{h\nu} (h\nu - E_g)^{1/2}, \quad (3)$$

where α is the absorption coefficient, $h\nu$ is the the photon energy, E_g is the energy gap and A is the constant depending on the type of transition. From (3), any energy can be rearranged and written in the form,

$$(\alpha h\nu)^2 = A^2(h\nu - E_g). \quad (4)$$

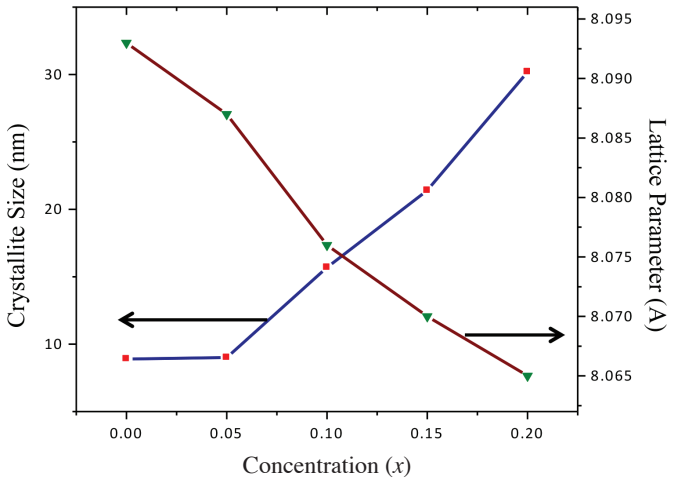

FIGURE 2. Crystallite size and lattice parameter of $Ca_xZn_{(1-x)}Al_2O_4$ with different concentration

TABLE 1. Structural parameters of $Ca_xZn_{(1-x)}Al_2O_4$ thin films

Concentration (x)	D (nm)	a (Å)	hkl	2θ (°C)	Apparent Density (g/cm^3)
0.00	8.9	8.093	311	36.24	4.59
0.05	9.0	8.087	311	36.25	4.60
0.10	15.7	8.076	311	36.26	4.62
0.15	21.4	8.070	311	36.27	4.63
0.20	30.2	8.065	311	36.28	4.64

From (4), it is clear when $h\nu = 0$, $Eg = h\nu$. The energy gap is determined by plotting $(\alpha h\nu)^2$ against $h\nu$ and finding the intercept on the $h\nu$ axis by extrapolating the plot to $(\alpha h\nu)^2 = 0$. The E_g of undoped Ca was determined to be 3.8 eV (Figure 3(a)), which is similar with those reported by Muhammad et al. (2011) and Zhang et al. (2012). However, the E_g decreased due to Ca-loading from 3.75 eV ($x = 0.05$) to 3.55 eV as shown in Figure 3. This is the first reported band gap of $CaZnAl_2O_4$. The E_g of $CaZnAl_2O_4$ less than 3.8 eV might be the result from the effect of the Ca bandgap (3.2 eV) or CaZnO (3.24 eV) (Xavier et al. 2009). In addition, the E_g decrease due to increase of intermediary energy levels within the optical band gap. Based on this information, it is possible to suggest that the E_g value of the Ca-content are associated with the contribution of intermediary energy levels of both $ZnAl_2O_4$ and Ca phases (Figure 3(b) to 3(d)). We suggest that the ideal E_g of $CaZnAl_2O_4$ is in range of 3.55 to 3.80 eV. Muhammad et al. 2011 reported that, the decrease in E_g can increase a.c. conductivity which is suitable for patch antenna.

MORPHOLOGY OBSERVATION

The micrograph images of $Ca_xZn_{(1-x)}Al_2O_4$ with $x = 0.00$, 0.05, 0.10, 0.15 and 0.20 are shown in Figure 4. The images of the film showed are small and large particles in stacked particle structure. The stacked particle was actually based on the concept of filling the pores by smaller size sphere between the large particles. The porosity between the small spheres was then filled up with still smaller spheres in order to give good particle stacking (Nikumbh & Adhyapak 2010). The images show the surface morphology of the layers depends on Ca- content. The samples show the morphology is sphere-like nanostructure. The grain size of undoped sample is in the range of 33 to 78 nm. The SEM shows the formation of soft agglomerates composed of fine nanoparticles. The presence of agglomerate displayed irregular morphology on the surface. The presence of agglomerates showed that the ZnO was not fully doped with Al_2O_3 as indicated from the XRD results. It will give nanostructural defects in the fired bodies, as it was detrimental to the mechanical properties of the material (Nikumbh & Adhyapak 2010).

SEM micrographs Figure 4(b) to 4(e) show the structure of $CaZnAl_2O_4$ with no more agglomerate appearing. The grain size increased up to 123 nm as x increased. Furthermore, the number of pores also decreased as the grain size increased by filling up with small particle. The increase of grain size is parallel with increase of crystallite

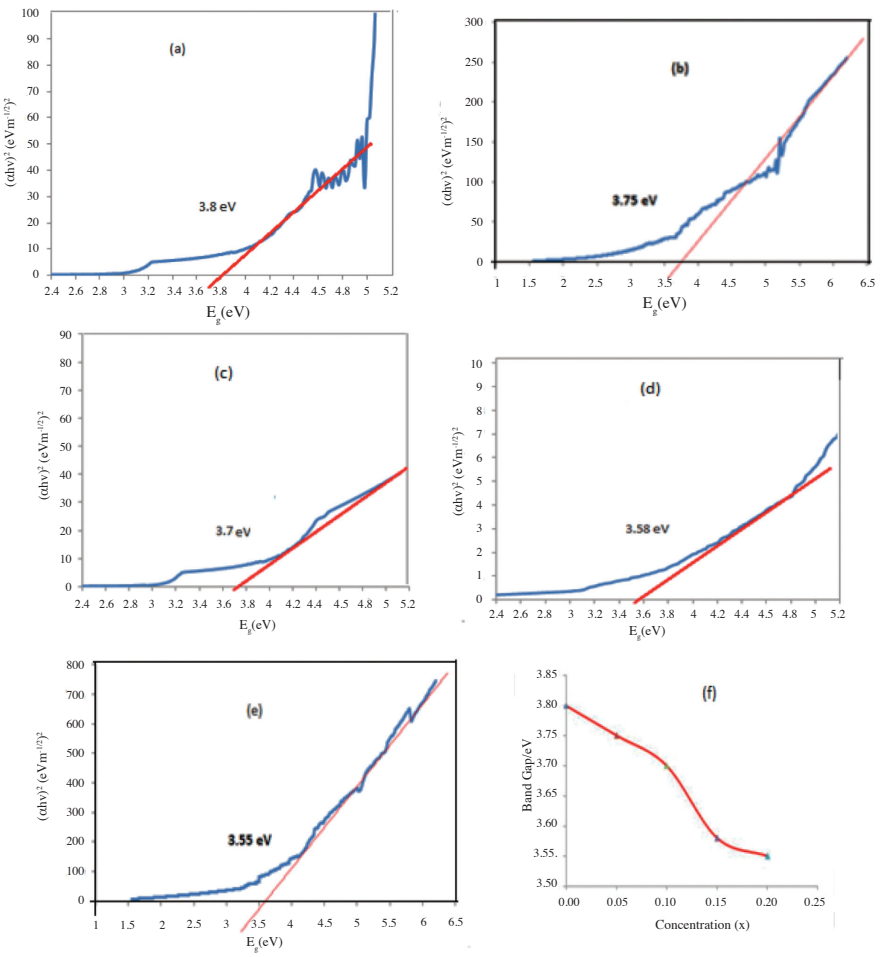

FIGURE 3. UV-vis absorbance spectra of $Ca_xZnAl_2O_4$;(a-e) and bandgap (E_g) graph (f)

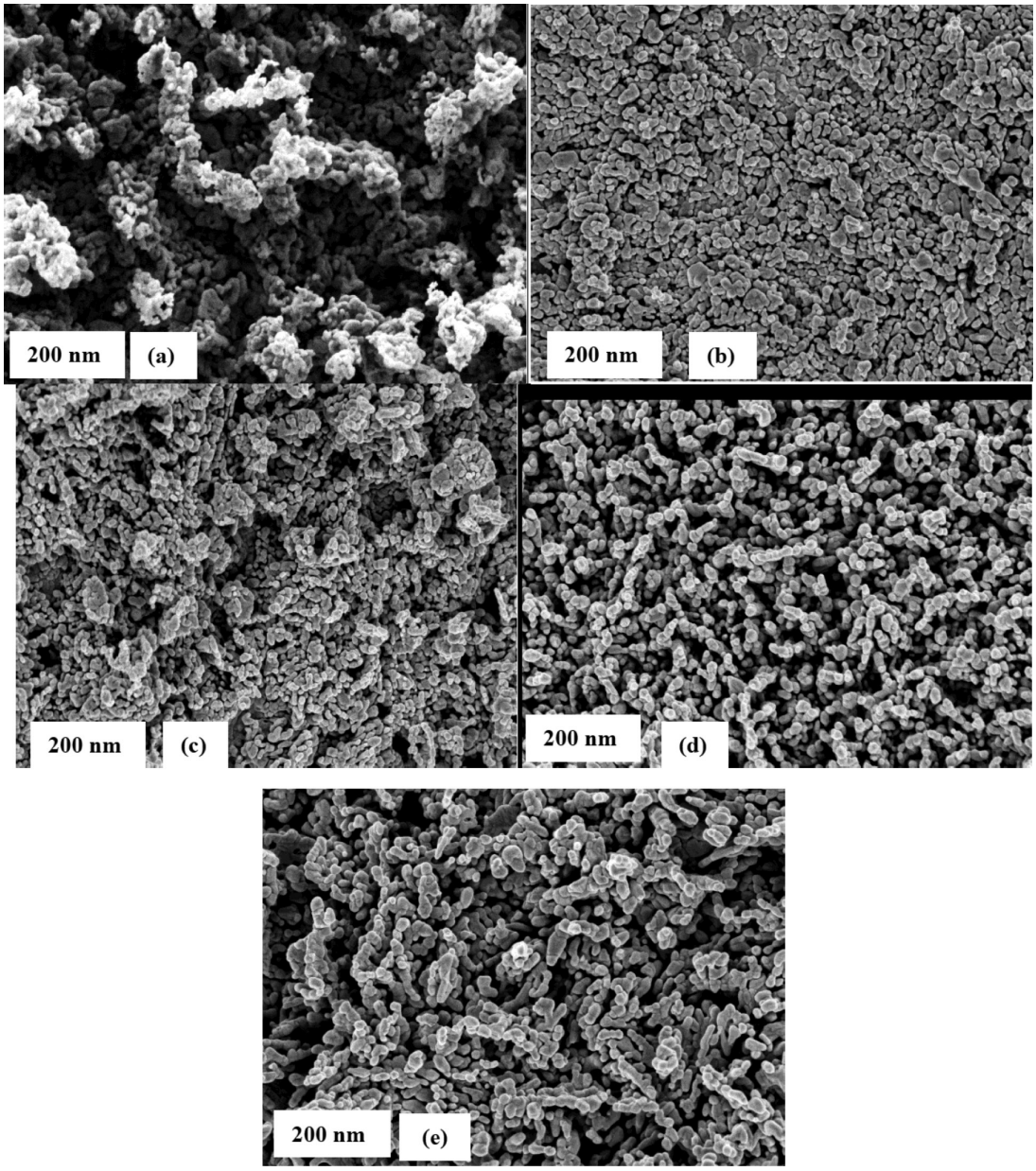

FIGURE 4. SEM micrographs of the different concentration $Ca_xZn_{(1-x)}Al_2O_4$ thin films, (a) x=0.00, (b) x=0.05, (c) 0.10, (d) 0.15 and (e) x=0.20

size in the XRD data. The EDX analysis of the $CaZnAl_2O_4$ sample is further demonstrated in the Figure 5. The EDX spectrum presented in Figure 5(a) for undoped Ca confirmed there was no Ca presence on the sample. The EDX analysis further confirmed that these thin films only contain Zn, Al and O, with their amount being 79.3, 20.04 and 0.63%, respectively. The Ca element was present when Ca was added. We found that the different Ca loading has changed the exact quantitative element of Zn, Ca, Al and O (Figure 5(b) to 5(e)). In order to estimate the thickness of the 10-layered film, the fractured cross-section of the substrate was imaged by SEM (Figure 6). Recently, Renata and Osvaldo (2010) reported that the size of the particles forming should be less than the thickness of thin film. The thickness of $ZnAl_2O_4$, $Ca_{0.05}Zn_{0.95}Al_2O_4$, $Ca_{0.10}Zn_{0.90}Al_2O_4$, $Ca_{0.15}Zn_{0.85}Al_2O_4$ and $Ca_{0.20}Zn_{0.80}Al_2O_4$ thin films were observed as 538, 656, 670, 902 and 971 nm, respectively. It enables us to infer that each deposited layer has a thickness of approximately 53.8, 65.6, 67.0, 90.2 and 97 nm. From this value, we can conclude that the size of the particles forming in thin film should be less than the thickness. The thickness of the films also increases with the increase of Ca- loading, due to increasing of grain size as calculated in SEM data.

The atomic force microscopy (AFM) was used to analyze the surface morphology of $Ca_xZn_{(1-x)}Al_2O_4$ as shown in Figure 7(a) to 7(e). The scanning size was 1 × 1 μm_2. The agglomerates (ZnO) also appeared on surface morphology, which is in agreement with (SEM) image and XRD data. The doped samples were identified as rough

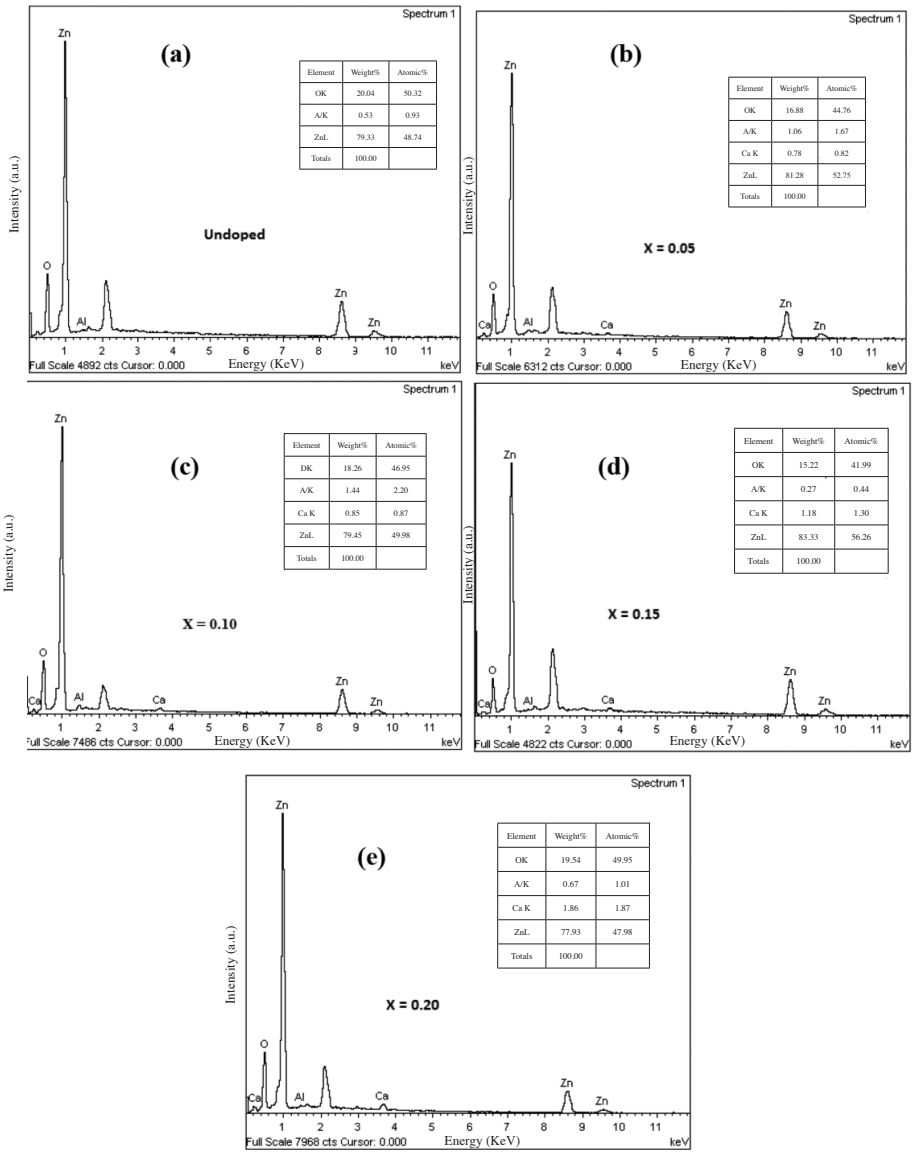

FIGURE 5. The EDX analysis of $Ca_xZn_{(1-x)}Al_2O_4$ (a) undop, (b) $x = 0.05$, (c) $x = 0.10$, (d) $x = 0.15$ and (e) $X = 0.20$

surface compared to $ZnAl_2O_4$ (Figure 7(a)) due to the fact that grain and crystallite size were increased. Furthermore, the increase of surface roughness can promote the increment of ceramics density and εr (Zhang Hui et al. 2005). The roughness average was increased linearly upon the Ca-content from 37.28 to 120.14 nm as shown in Figure 7(f).

DIELECTRIC CONSTANT

Figure 8 shows the variation in dielectric constant (ε_r) of films with applied frequency (20 Hz to 1 MHz) at room temperature. There is a steady decrease in ε_r value within an applied frequency. This phenomenon can be understood on the basis of Maxwell–Wagner model of interfacial polarization and Koop's phenomenological theory (Koops 1951; Wagner 1993). The ε_r was calculated from the values of capacitance using the relation (Muhammad et al. 2011);

$$\varepsilon' = Cd/\varepsilon oA', \quad (5)$$

where ε' is the dielectric constant of the sample (the real part), C the capacitance of the capacitor formed by inserting the sample between two metal plates, d the thickness of the sample, ε_o the permittivity of free space and A the area of cross section of the sample. It can be observed that the ε_r value of un-doped sample was 8.48, which is in good agreement with previous results reported by Lei et al. (2011) (ε_r~8.3) and Surendran et al. (2004) (ε_r~8.5). The addition of Ca improved the ε_r from 8.57 to 9.54. The increasing of ε_r values follow the logarithmic mixing rule (Kingery et al. 1976); $\ln \varepsilon_r = v1 \ln \varepsilon_r 1 + v2 \ln \varepsilon_r 2$ where εr1 and εr2 are the dielectric constants of phases with volumes $v1$ and $v2$. According to Subramanian et al. (1989), the dielectric constant of calcium is 11.95, so it is able to increase the εr of $Ca_xZn_{(1-x)}Al_2O_4$. Figure 9 shows the relationship between ε_r and apparent density with the x value. Based on the material investigated above and

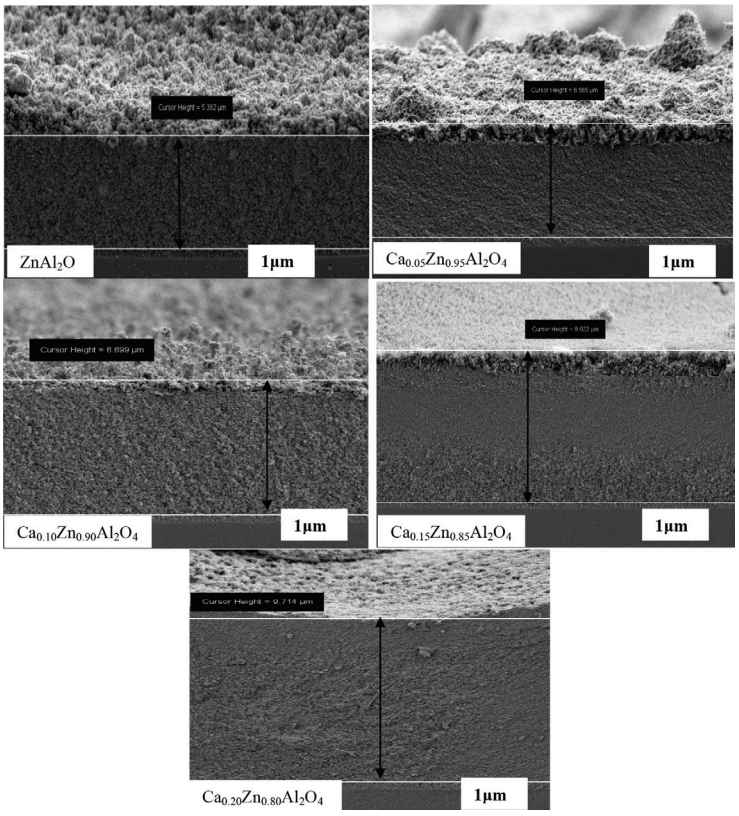

FIGURE 6. Cross-section by SEM of the 10-layered $Ca_xZn_{(1-x)}Al_2O_4$ thin films

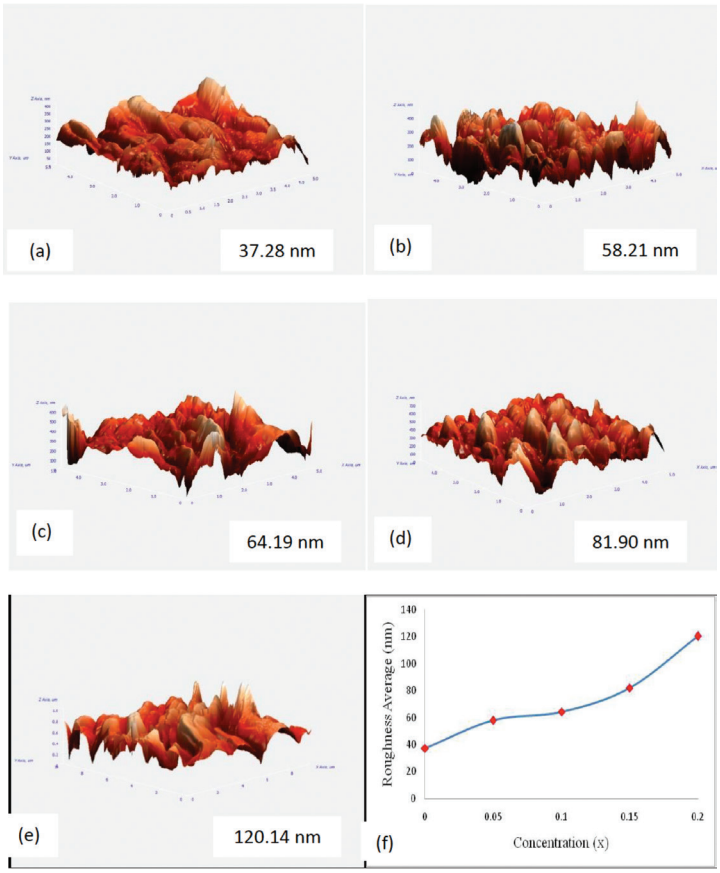

FIGURE 7. AFM images of $Ca_xZn_{(1-x)}Al_2O_4$ thin films with different concentration (a) – (e) and roughness average of $Ca_xZn_{(1-x)}Al_2O_4$ (f)

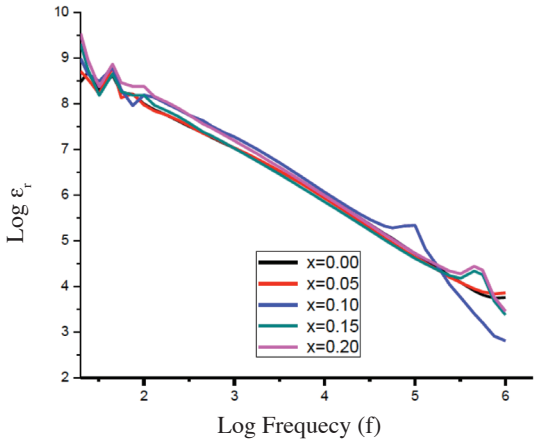

FIGURE 8. Variation in dielectric constant (ε_r) of $Ca_xZn_{(1-x)}Al_2O_4$ thin films

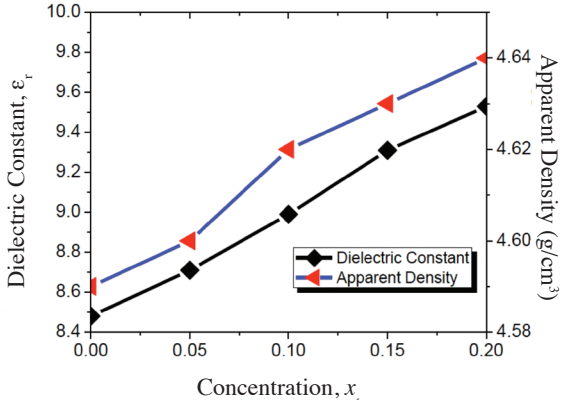

FIGURE 9. Apparent density and dielectric constants of $Ca_xZn_{(1-x)}Al_2O_4$ ceramics with different concentration (x)

microwave antenna theory, a microstrip patch antenna for GPS application is able to be fabricated using the $Ca_xZn_{(1-x)}Al_2O_4$.

CONCLUSION

The $Ca_xZn_{(1-x)}Al_2O_4$ thin films (x = 0.0; 0.10, 0.15 and 0.20) were synthesized by the sol-gel method. The XRD patterns and EDX analysis confirmed that nanostructures of Ca-Zn-Al_2O_4 were observed. The XRD data also showed that diffraction peaks of all samples corresponded to the standard pattern of face-centred cubic (fcc) structure. The measured bandgap of undoped and high doping (x = 0.20) changed from 3.8 to 3.55 eV. The XRD data showed that diffraction peaks of highest doping (x = 0.20) corresponded to the standard pattern of face-centered cubic $ZnAl_2O_4$ with dominant peak 311. XRD and SEM results showed that the crystallite and grain size increased as the Ca-loading increased. The substitution of Zn^{2+} by

Ca^{2+} in the $ZnAl_2O_4$ thin film increased the crystallite size, grain size and surface roughness which evidently affects their density and dielectric properties, making the material, a candidate for GPS patch antennas. The increase in apparent densities contributed to the increment of dielectric constant and plays an important role in order to miniaturize GPS patch antennas. Therefore, the $CaZnAl_2O_4$ microwave dielectric ceramics are suitable for GPS patch antennas.

ACKNOWLEDGEMENTS

This project was fully carried out in the Photonic Technology Laboratory, Institute of Microengineering and Nanoelectronics (IMEN), Universiti Kebangsaan Malaysia, Malaysia under grant UKM-GUP-2011-056.

REFERENCES

Barros, B.S., Melo, P.S., Kiminami, R.H.G.A., Costa, A.C.F.M., de Sa, G.F. & Alves Jr. S. 2006. Photophysical properties of Eu3+ and Tb3+-doped $ZnAl_2O_4$ phosphors obtained by combustion reaction. *Journal of Material Science* 41: 4744-4748.

Bian, J.J., Yan, K. & Dong, Y.F. 2008. Microwave dielectric properties of A1-3x/2 La x (Mg ½) 0 3 (A = Ba, Sr, Ca; 0.0 < 0.05) double perovskites. *Materials Science and Engineering B – advanced Functional Solid-State Materials* 147(1): 27-34.

Chatpong Bangbai, Krisana Chongsri, Wisanu Pecharapa & Wicharn Techitdheera. 2013. Effect of Al and N doping on structural and optical properties of sol-gel derived ZnO thin films. *Sains Malaysiana* 42: 239-246.

Chen, Y-C. 2011. Microwave dielectric properties of (Mg(1–*x*) Co*x*)2SnO4 ceramics for application in dual-band inverted-e-shaped monopole antenna. *IEEE Transactions on Ultrasonics, Ferroelectrics, and Frequency Control* 58: 2531-2538.

Ciupina, V., Carazeanua, I. & Prodan, G. 2004. Characterization of ZnAl2o4 nanocrystals prepared by coprecipitation and microemulsion techniques. *Journal of Optoelectronics and Advanced Materials* 6: 1317-1322.

de Souza, L.K.C., Zamian, J.R., da Rocha Filho, G.N., Soledad, L.E.B., dos Santos, I.M.G., Souza, A.G., Scheller, T., Angelica, R.S. & da Costa, C.E.F. 2009. Blue pigments based on $Co_xZn_{1-x}Al_2O_4$ spinels synthesized by the polymeric precursor method. *Dyes and Pigments* 81: 187-192.

Farley, N.R.S., Staddon, C.R., Zhao, L.X., Edmonds, K.W., Gallagher, B.L. & Gregory, D.H. 2003. New sol-gel synthesis of ordered nanostructured doped ZnO films. *J. App. Phys.* 93: 1-8.

Fatemeh Davara & Masoud Salavati-Niasaria. 2011. Synthesis and characterization of spinel- type zinc aluminate nanoparticles by a modified sol-gel method using new precursor. *Journal of Alloys and Compounds* 509: 2487-2492.

Fauzana, A.N., Azmi, B.Z., Sabri, M.G.M., Wan Abdullah, W.R. & Hashim, M. 2013. Microstructural and nonlinear electrical properties of ZnO ceramics with small amount of MnO_2 dopant. *Sains Malaysiana* 42: 1139-1144.

Huang, C-L., Chen, J-Y. & Li, B-J. 2009. Characterization and dielectric behavior of a new dielectric ceramics Ca(Mg1/3Nb2/3)O3–(Ca0.8Sr0.2)TiO_3 at microwave frequencies. *J. of Alloys and Compounds* 484: 494-497.

Huang, C-L., Chen, J-Y. & Wang, Y-H. 2009. Microwave dielectric properties of (Mg0.95Co0.05)TiO_3-(Na0.5Nd0.5) TiO_3 ceramic system. *J. of Alloys and Compounds* 478: 842-846.

Huang, C-L., Yang, T-J. & Huang, C-C. 2009. Low dielectric loss ceramics in the $ZnAl_2O_4$–TiO_2 system as a τf compensator. *J. of the American Ceramic Society* 92: 119-124.

Hui Zhang, Liang, Fang, Elsebrock, R. & Yuan, R.Z. 2005. Crystal structure and microwave dielectric properties of a new $A_6B_5O_{18}$-type cation-deficient perovskite $Ba_3La_3Ti_4NbO_{18}$. *Materials Chemistry and Physics* 93: 450-454.

Ianos, R., Lazau, R., Lazau, I. & Pacurariu, C. 2011. Chemical oxidation of residual carbon from $ZnAl_2O_4$ powders prepared by combustion synthesis. 2012. *J. of the European Ceramic Society* 32: 1605-1611.

Kingery, W., Bowen, H. & Uhlmann, D. 1976. *Introduction to Ceramics*. John Willey & Son, New York.

Koops, C.G. 1951. On the dispersion of resistivity and dielectric constant of some semiconductors at audio frequencies. *Physics Review* 81: 121-124.

Lei, W., Lu, W-Z., Wang, X-H., Liang, F. & Wang, J. 2011. Phase composition and microwave dielectric properties of $ZnAl_2O_4$–Co_2TiO_4 low-permittivity ceramics with high quality factor. *J. of the American Ceramic Society* 94: 20-23.

Lei, W., Lu, W-Z., Liu, D. & Zhu, J-H. 2009. Phase evolution and microwave dielectric properties of $(1–x)ZnAl_2O_4$–x Mg_2TiO_4 ceramics. *Journal of the American Ceramic Society* 92: 105-109.

Muhammad E. Abdul Jamal, Sakthi Kumar D. & Anantharaman, M.R. 2011. On structural, optical and dielectric properties of zinc aluminate nanoparticles. *Bull. Mater. Sci*.34: 251-259.

Narang, S.B. & Shalini, B. 2010. Low loss dielectric ceramics for microwave applications: A review. *Journal of Ceramic Processing Research* 11: 316-321.

Nikumbh, A.K. & Adhyapak, P.V. 2010. Synthesis, properties and optimization of the rheologicalbehaviors on alumina and zinc aluminate powders obtain from dicarboxylate precursors. *Powder Technology* 202: 14-23.

Renata, F.M. & Osvaldo, A.S. 2010. Thin film of $ZnAl_2O_4$: Eu^{3+} synthesized by a non-alkoxide precursor sol-gel method. *Journal of Brazil Chemistry Society* 21: 1395-1398.

Rodríguez, M.A., Aguilar, C.L. & Aghayan, M.A. 2012. Solution combustion synthesis and sintering behavior of $CaAl_2O_4$. *Ceramics International* 38: 395-399.

Saberi, A., Golestani-Fard, F., Sarpoolaky, H., Willert-Porada, M., Gerdes, T. & Simon, R. 2008. Chemical synthesis of nanocrystalline magnesium aluminate spinel via nitrate- citrate combustion route. *Journal of Alloy Compound* 462: 142-146.

Sanchez, R.D., Saleta, M.E., Shapoval, O., Gehrke, K., Moshnyaga, V. & Samwer, K. 2010. Characterization of geometrically frustrated $Zn_{1-x}MnxAl_2O_4$ thin films prepared by metalorganic aerosol deposition. *Journal of Physics: Conference Series* 200: 1-4.

Sebastian, M.T. 2008. *Dielectric Materials for Wireless Communication*. Jordan Hill, Oxford, UK: Elsevier Ltd.

Subramanian, M.A., Shannon, R.D., Chai, B.H.T., Abraham, M.M. & Wintersgill, M.C. 1989. Dielectric constants of BeO, MgO, and CaO using the two-terminal method. *Phys. Chem. Minerals* 16: 741-746.

Surendran, K.P., Santha, N., Mohanan, P. & Sebastian, M.T. 2004. Temperature stable low loss ceramic dielectrics in (1-x) $ZnAl_2O4$-$xTiO_2$ system for microwave substrate applications. *The European Physical Journal B* 41: 301-306.

Suresh K Sampath, D.G. Kanhere & Ravindra Pandey. 1999. Electronic structure of spinel oxides: Zinc aluminate and zinc gallate. *J. Phys. Condens. Matter.* 11: 3635-3644.

Tawatchai Charinpanitkul, Pattama Poommarin, Akkarat Wongkaew & Kim, K-S. 2009. Dependence of zinc aluminate microscopic structure on its synthesis. *Journal of Industrial and Engineering Chemistry* 15: 163-166.

Thinesh Kumar, R., Clament Sagaya Selvam, N., Ragupathi, C., John Kennedy, L. & Judith Vijaya, J. 2012. Synthesis, characterization and performance of porous Sr(II)-added $ZnAl_2O_4$ nanomaterials for optical and catalytic applications. *Powder Technology* 224: 147-154.

Tian, X., Wan, L., Pan, K., Tian, C., Fu, H. & Shi, K. 2009. Facile synthesis of mesoporous $ZnAl_2O_4$ thin films through the evaporation-induced self-assembly method. *Journal of Alloys and Compounds* 488(1): 320-324.

Wagner, K.W. 1913. Zur theorie der unvollkommenen dielektrika. *Annalen der Physik* 345: 817-855.

Wang, X.C., Lei, W. & Lu, W.Z. 2009. Novel ZnAI204-based microwave dielectric ceramics with machinable property and its application for GPS antenna. *Ferroelectrics* 388: 80-87.

Wood, D.L. & Tauc, J. 1972. Weak absorption tails in amorphous semiconductors. *Phys. Rev. B* 5: 3144-3151.

Wu, J-M., Lu, W-Z., Lei, W. & Wang, X-C. 2011. Preparation of $ZnAl_2O_4$-based microwave dielectric ceramics and GPS antenna by aqueous gelcasting. *Materials Research Bulletin* 46: 1485-1489.

Xavier, C.S., Sczancoski, J.C., Cavalcante, L.S., Paiva-Santos, C.O., Varela, J.A., Longo, E. & Li, M.S. 2009. A new processing method of CaZn2(OH)6.2H_2O powders: Photoluminescence and growth mechanism. *Solid State Sciences* 11: 2173-2179.

Ye, X., Wen, W.L. & Lu, W-Z. 2009. Microwave dielectric characteristics of Nb2O5-added 0.9Al2O3–0.1TiO_2 ceramics. *Ceramics International* 35: 2131-2134.

Zawadzki, M., Staszak, W., López-Suárez, F.E., Illán-Gómez, M.J. & Bueno-López, A. 2009. Preparation, characterisation and catalytic performance for soot oxidation of copper- containing $ZnAl_2O_4$ spinels. *Applied Catalysis A: General* 371: 92-98.

Zhang, D., Wang, C., Liu, Y., Shi, Q., Wang, W. & Zhai, Y. 2012. Green and red photoluminescence from $ZnAl_2O_4$: Mn phosphors prepared by sol-gel method. *Journal of Luminescence* 132: 1529-1531.

Wan Nasarudin Wan Jalal, Huda Abdullah*,
Mohd Syafiq Zulfakar & Badariah Bais
Department of Electrical, Electronic and System Engineering
Faculty of Engineering and Built Environment
Universiti Kebangsaan Malaysia
43600 Bangi, Selangor
Malaysia

Sahbudin Shaari
Institute of Microengineering and Nanoelectronics (IMEN)
Universiti Kebangsaan Malaysia
43600 Bangi, Selangor
Malaysia

Mohammad Thariqul Islam
The Institute of Space Science (ANGKASA)
Universiti Kebangsaan Malaysia
43600 Bangi, Selangor
Malaysia

*Corresponding author; email: huda@vlsi.eng.ukm.edu.my

Received: 28 March 2013
Accepted: 2 February 2014